



Biodegradable poly(butylene adipate-co-terephthalate)/poly(vinyl acetate) blends with improved rheological and mechanical properties

Ye Zhang¹ · Lijuan Wang¹ · Changyu Han²

Received: 21 November 2021 / Accepted: 22 March 2022 / Published online: 7 April 2022
© The Polymer Society, Taipei 2022

Abstract

Poly(butylene adipate-co-terephthalate) (PBAT) are expected to be widely used for production of biodegradable film materials. However, poor rheological properties, low yield strength and modulus of PBAT limit its applications in some field. Herein, PBAT/poly(vinyl acetate) PVAc blends were prepared by melt mixing to overcome aforementioned shortcomings. The miscibility, phase morphology, thermal properties, rheological properties and mechanical properties of PBAT/PVAc blends were studied. Miscibility analysis showed that PBAT/PVAc blends were immiscible two-phase system. The uniform dispersion of PVAc in PBAT matrix was observed in SEM images. From thermal properties analysis, the incorporation of PVAc accelerated crystallization rate and enhances crystallization ability of PBAT. Rheological analysis demonstrated that storage modulus, loss modulus and complex viscosity of PBAT were obviously improved when PVAc was added due to the high viscosity of PVAc in melt state. Mechanical data indicated incorporation of PVAc could enhance modulus and yield strength of PBAT. When the content of PVAc was 30%, Young's modulus and yield strength of PBAT were improved about 105% (from 203 to 416 MPa) and 53.3% (from 7.5 to 11.5 MPa), respectively. In addition, the elongation at break and tensile strength of blends decreased with the increase in PBAT loading, but all the PBAT/PVAc blends maintained the elongation at break of more than 700%, which meets the requirements of most applications.

Keywords Poly(butylene adipate-co-terephthalate) · Poly(vinyl acetate) · Blend · Miscibility

Introduction

The widespread application of plastic products in various industries has provided great convenience to the development of social economy because of the light quality, easy processing, corrosion resistance and other advantages of plastic products. However, the large-scale production and consumption of plastic products have generated a series of issues in recent years such as significant environmental concerns, waste plastics management and carbon emissions [1]. With the tremendous attention to environmental conservation,

the development and application of biodegradable polymers that can substitute for conventional non-biodegradable polymers have recently gaining considerable attention from both industry and academia. Biodegradable polymers are environment-friendly materials and can be easily decomposed into small molecules upon disposal in bioactive environments by microorganisms, such as bacteria, algae, and fungi, etc., or by hydrolysis in buffer solutions or sea water in a certain period of time [1–3]. Biodegradable polymers are usually classified into bio-based biodegradable polymers and petrochemical-based biodegradable polymers. Bio-based biodegradable polymers are further divided into two categories: natural synthetic biodegradable polymers and chemical synthetic biodegradable polymers. The former category refers to organic chemical polymers formed in the natural environment, such as natural rubber [4], starch [5], chitin, protein, agar, cellulose and natural lignin, etc. The latter category refers to the polymers obtained through the participation of microorganisms, mainly including poly(lactic acid) (PLA) [6–10] and poly(hydroxyalkanoate)s (PHAs) [11, 12]. Petroleum-based biodegradable polymer refers to the polymer

✉ Lijuan Wang
wanglj15@ccut.edu.cn

✉ Changyu Han
cyhan@ciac.ac.cn

¹ School of Chemical Engineering, Changchun University of Technology, Changchun 130012, China

² Key Laboratory of Polymer Ecomaterials, Chinese Academy of Sciences, Changchun Institute of Applied Chemistry, Changchun 130022, China

obtained by the polymerization of monomers of petrochemical products by chemical synthesis method, mainly containing poly(ϵ -caprolactone) (PCL) [13–15], poly(butylene succinate) (PBS) [16, 17], poly(butylene adipate-co-terephthalate) (PBAT) [18–20], poly(glycolic acid) (PGA) [21, 22] and poly(propylene carbonate) (PPC) [23, 24], etc.

Among these various biodegradable polymers, in particular, PBAT is a commercialized aliphatic–aromatic copolyester from petrochemical resources and could be produced through transesterification and polycondensation reaction of 1,4-butanediol, adipic acid and terephthalic acid [25, 26]. Apart from its biodegradability, PBAT shows a significant amount of merits including competitive flexibility, high strength, high resilience, thermal processability, good tear resistance, excellent sealing performance and biocompatibility [27, 28]. With these excellent properties, PBAT becomes an ideal substitute for non-biodegradable plastics, used as packaging materials, medical devices, agricultural mulching films, building panels and foam materials. However, some disadvantages such as poor rheological properties, low yield strength and modulus of PBAT cannot fulfill the requirements in numerous plastic products and limits its widespread applications. Blending PBAT with other materials is undoubtedly a simple, economic and cost-effective solution to address these issues. Hence, PBAT is usually applied in the form of composite materials. PBAT/PLA blends have received considerable research attention on the basis of that the blends could counteract the weaknesses of each of its components and composite with excellent comprehensive performance can be obtained [29–31]. The abundant and renewable polymer starch is deemed as ideal candidate that could be incorporated into the formulation with the aim of reducing the production costs. Many researches focused on the PBAT/starch blends have been reported so far [32–35]. Other polymers such as PPC, PBS, PCL, PGA, poly(hydroxybutyrate-co-hydroxyvalerate) (PHBV), poly(trimethylene terephthalate) (PTT), poly(vinyl chloride) (PVC), polycarbonate (PC),

polypropylene (PP), and natural rubber are also used to blend with PBAT to improve the properties of composites [27, 36–44]. In addition, the utilization of inorganic materials (talc, montmorillonite, and calcium carbonate etc.) as additives is a common yet effective method to improve the properties of PBAT [45].

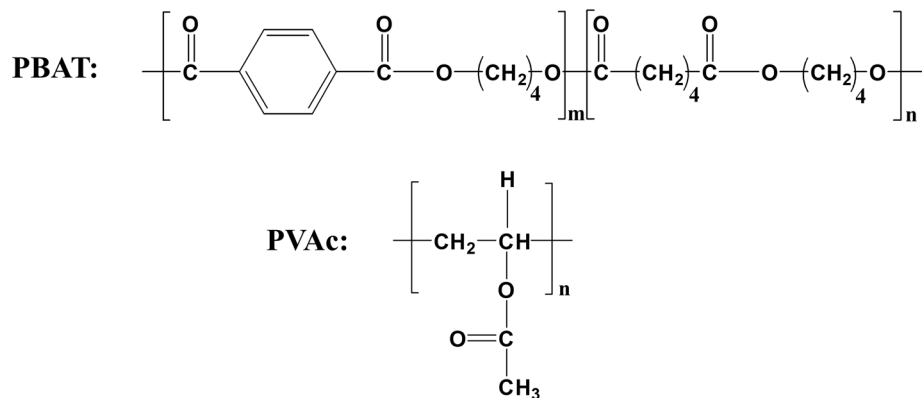
Poly(vinyl acetate) (PVAc) is a typical thermoplastic amorphous polymer with high modulus. In recent years, PVAc has been exploited for a multiplicity of many applications, such as paints, tissue engineering, surface coatings, electrode binder, food additives and glues for wood, paper and cloth [46]. Blends of PVAc with other polymers have attracted much attention, including poly(ethylene oxide) (PEO) [47], PCL [48], PLA [49], PBS [50], poly(methyl methacrylate) (PMMA) [51], and poly(3-hydroxy butyrate) (PHB) [52] etc. Therefore, to exploit new biodegradable blend systems, counteract the weaknesses of PBAT and PVAc, and develop composite with balanced performance, a set of the PBAT/PVAc blends with different PVAc loadings were fabricated through melt processing in this work. Miscibility, morphology, thermal behaviors, rheological properties, and mechanical properties of the blends were investigated using various analytical methods.

Experimental

Materials

Commercially available PBAT used in this work was provided by Xinjiang Blue Ridge Tunhe Polyester Co., Ltd in pellet form with the weight-average molecular weight (M_w) of $1.50 \times 10^5 \text{ g mol}^{-1}$ and polydispersity (M_w/M_n) of 1.45, respectively. PVAc with M_w of $4.8 \times 10^5 \text{ g mol}^{-1}$ and polydispersity of 1.21 was purchased from Aldrich. Figure 1 shows the chemical structures of PBAT and PVAc.

Fig. 1 Chemical structures of PBAT and PVAc



Sample preparation

Prior to the processing, PBAT and PVAc pellets without further purification were dried at 50 °C for 6 h using a vacuum oven in order to remove the moisture and prevent hydrolysis. The PBAT/PVAc weight ratios of blends were fixed at 100/0, 90/10, 80/20, 70/30, and 0/100 w/w and neat PBAT, PBAT-10, PBAT-20, PBAT-30 and neat PVAc were used to represent corresponding blends respectively in the following testing and analysis. The PBAT/PVAc blends were melt-compounded using a Haake Rheomix 600 (Karlsruhe, Germany). The rotation speed was set to 60 rpm and melt blending time was maintained for 300 s at 150 °C. After compounding, all of the blends were cut into small pellets. Then, all the prepared blends were compression-molded to obtain the sheets with thicknesses of 1.0 mm under the optimum conditions: at a pressure of 10 MPa and 160 °C for 2 min. Subsequently, the sheets for various tests were quenched to room temperature. Finally, the sheets were cut into dumbbell shape with a width of 4 mm and a length of 20 mm for mechanical properties test and into rectangles with a width of 4 mm and a length of 20 mm for dynamic mechanical test and into round shape with a diameter of 25 mm for rheological test.

Characterization

Dynamic mechanical analysis

Dynamic mechanical properties of the blends were studied with a DMA instrument (DMA 850, TA Instrument, Co., USA) using the rectangular sheets previously cut. Test was carried out in the tensile mode with temperature ranging from -60 to 80 °C. The constant oscillating frequency and strain amplitude of the test were set to be 1 Hz and 20 μm , respectively. The heating rate was 3 °C min^{-1} .

Scanning electron microscopy (SEM)

The microstructure of the blends was investigated by a scanning electron microscope (SEM) (Model JSM6400, JEOL, USA) at an accelerating voltage of 10 kV. Firstly, the prepared rectangular blend sheet specimens mentioned in sample preparation were submerged in liquid nitrogen for 20 min, and then immediately fractured to obtain the cryofractured surfaces. Finally, the cryofractured specimens were etched by acetone solution to remove the PVAc phase for the purpose of better phase structure observation. The cryofractured specimens were glued on a copper stand and the fracture surfaces were gold sputter-coated before

morphological observation. In the SEM images, the scales of 2 and 10 μm corresponded to magnifications of 8000 \times and 2000 \times , respectively.

Differential scanning calorimetry (DSC)

Thermal properties of neat PBAT, neat PVAc, and the PBAT/PVAc blends were studied using a differential scanning calorimetry (TA Instruments DSC Q20 USA) under nitrogen atmosphere with a gas flow rate of 50 ml min^{-1} . The samples sliced from compression-molded sheets (about 5 to 8 mg) were sealed in an aluminum pan by crimping and heated to 150 °C. Then the samples were equilibrated for 3 min at 150 °C in order to removing the heating history. Finally, the samples were cooled down to -50 °C and reheated again to 150 °C. The heating and cooling rates were set to 10 °C min^{-1} . The thermal parameters including glass transition temperature (T_g), crystallization temperature (T_c), melting temperature (T_m), crystallization enthalpy (ΔH_c), melting enthalpy (ΔH_m) and degree of crystallinity (X_c) were determined from DSC scanning thermograms.

Rheological measurements

Melt rheological properties of PBAT/PVAc blends were conducted by using a parallel plate rheometer (AR 2000ex, TA, USA) in dynamic flow field. Precutted round shape sheets with a diameter of 25 mm and thickness of about 1 mm were placed between the plates with diameter of 25 mm. Frequency sweep tests were done at 150 °C in a frequency range from 0.05 to 100 rad s^{-1} under nitrogen atmosphere. To guarantee that the test was performed in the linear viscoelastic region, the strain value was set to 1.25%. The sample gap distance between the parallel plates was set as 0.95 mm.

Static tensile properties testing

The uniaxial tensile properties of the PBAT/PVAc blends were determined with an Instron 1211 testing machine according to ASTM D638-2008 standard. The dumbbell shape samples of the PBAT/PVAc blends punched out from the compression molded sheets were pre-conditioned for 24 h at room temperature and 50% relative humidity controlled environment prior to measurement. The crosshead speed of all tests was kept at 200 mm min^{-1} .

Results and discussion

Miscibility analysis of PBAT/PVAc blends

The dynamic mechanical analysis (DMA) is a feasible and very useful criterion for the determination of the miscibility

and interfacial interactions of polymer blends. The curves of $\tan\delta$ and storage modulus dependence on temperature for neat PBAT, neat PVAc and PBAT/PVAc blends are exhibited in Figs. 2 and 3, respectively. The maximum height value of the $\tan\delta$ peak representing the transition in molecular mobility is corresponded to the glass transition temperature (T_g). Generally, the immiscible blend system exhibits multiple $T_{g,s}$, which correspond to T_g of individual components in the blend system, while miscible blend system has a single T_g lying between the transition temperature of individual components with an increased broadness in the transition peak [53, 54]. The values of $T_{g,s}$ obtained from the peak temperature are listed in Table 1. It can be seen from Fig. 2 that neat PBAT and neat PVAc only exhibited one glass transition temperature at -25.2°C and 50.5°C , respectively. As for the PBAT/PVAc blends, two distinct $T_{g,s}$ were observed that correspond to the glass transitions of PBAT-rich phase and PVAc-rich domains, respectively. The lower temperature was attributed to the T_g of PBAT phase and the high temperature was attributed to the T_g of PVAc phase. In addition, with the increase of PVAc content, T_g of PBAT and PVAc in the binary blend did not change significantly. These observations can imply that PBAT was immiscible with PVAc and PBAT/PVAc blends were typical two-phase system with the presence of phase separation existing in the system [55].

From Fig. 3, it can be seen that storage modulus values showed a sharp decrease in the range of -35 to 20°C and 40 to 50°C respectively for neat PBAT and PVAc, which resulted from the occurrence of their glass transitions. As for the PBAT/PVAc blends, when the temperature was below about -35°C , the variation of PVAc content had no obvious effect on storage modulus value because both PBAT and PVAc were in a glassy state. At the temperatures between -35 and 40°C , the storage modulus of PBAT/PVAc blends

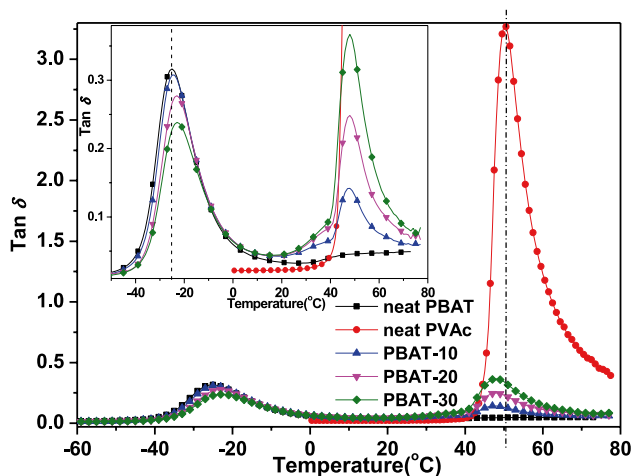


Fig. 2 The curves of $\tan\delta$ dependence on temperature for neat PBAT, neat PVAc and PBAT/PVAc blends

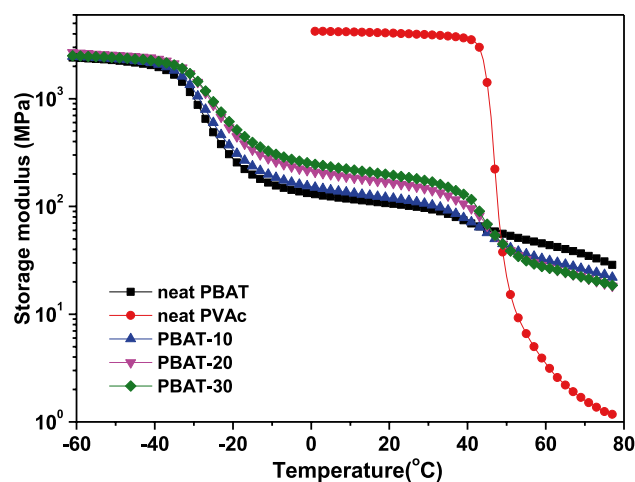


Fig. 3 The curves of storage modulus dependence on temperature for neat PBAT, neat PVAc and PBAT/PVAc blends

was gradually reinforced with the PVAc content increasing and the reinforcement of storage modulus could be attributed to the high stiffness of PVAc under glassy state. The storage modulus at room temperature (about 20°C) was 105 MPa for neat PBAT, which increased to 200 MPa for the PBAT/PVAc blend consisting of 30% PVAc ($\sim 90.4\%$ reinforcement). The reinforcement of storage modulus indicated that the movement of molecular chain needed more stress and the addition of PVAc could make up for low modulus of PBAT. Besides above 50°C , storage modulus of the PBAT/PVAc blend was higher than that of neat PVAc, and decreased when PVAc content increased. This was attributed to rubbery PVAc segments had excellent mobility.

Scanning electron microscopy (SEM) analysis

It is well recognized that phase morphology of polymer blend has an important effect on various properties of blend and can be obtained from scanning electron microscope (SEM). For miscible blends, uniform single-phase morphology usually can be observed and separate phase morphology can be observed for immiscible blends. In order to investigate phase morphology, the cryofractured surface images of the neat PBAT, neat PVAc, and PBAT/PVAc blends after

Table 1 $T_{g,s}$ of neat PBAT, neat PVAc, and PBAT/PVAc blends obtained from DMA

Sample	neat PBAT	PBAT-10	PBAT-20	PBAT-30	neat PVAc
T_{g-PBAT} ($^\circ\text{C}$)	-25.2	-24.6	-23.1	-22.7	-
T_{g-PVAc} ($^\circ\text{C}$)	-	47.4	47.9	48.1	50.5

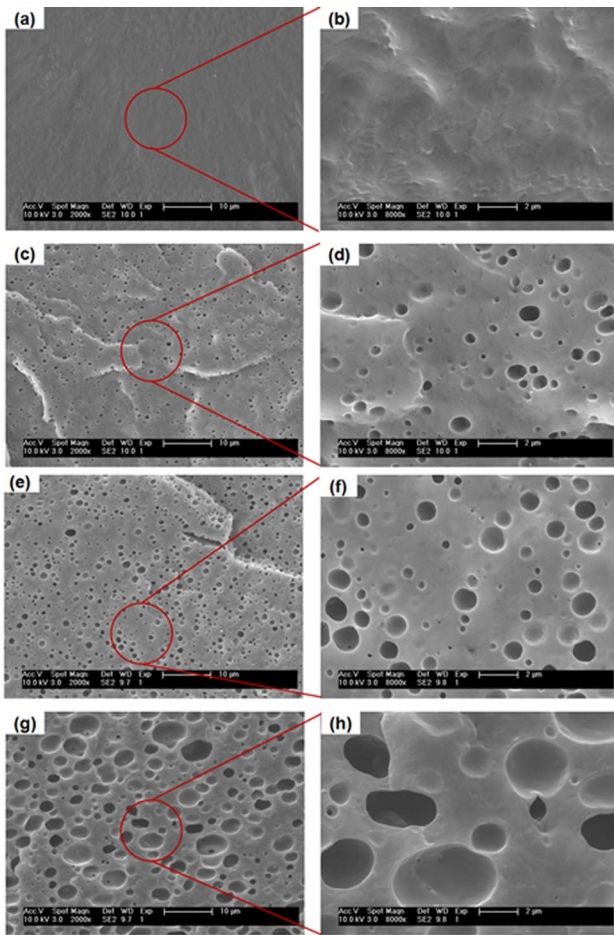


Fig. 4 SEM images of cryo-fractured surfaces of neat PBAT and PBAT/PVAc blends after etching PVAc: (a, b) neat PBAT, (c, d) PBAT-10, (e, f) PBAT-20, and (g, h) PBAT-30

etching PVAc were obtained by SEM and exhibited in Fig. 4. Among these images, Fig. 4b, d, f, and h were the magnified images of sectional cryofractured cross-section. As clearly presented in Fig. 4a, the cryofractured surface of neat PBAT showed single-phase morphology feature with very homogeneous and smooth surface. From Fig. 4c, e, and g, all PBAT/

PVAc blends showed a clear two-phase phase-separated morphology, which possessed typical sea-island structure, and this result was well consistent with the two T_g s measured by DMA analysis. The gray-white part in the images was assigned to the continuous PBAT matrix, and the dark phase parts corresponded to the round holes where etched PVAc located. Moreover, it was found that PVAc minor phase preferentially uniformly and discretely dispersed spherical droplets in the continuous PBAT matrix when the PVAc content did not exceed 30 wt%. What is noteworthy is that morphological variations were found depending on the blend composition. The average particle size and distribution of the PVAc was quantitatively analyzed by measuring the average maximum diameter (D_{max}), minimum average diameter (D_{min}), and average diameter (D) using Nano Measurer 1.2 software based on the SEM images. The particle size distributions were illustrated in Fig. 5. The D of the PVAc phase was approximately 0.56 μm when the PVAc content was 10 wt%. It was found that further raising PVAc loading, the D of PVAc phase increased. For example, D of PBAT/PVAc blends containing PVAc of 20 and 30 wt% were 0.76 and 2.51 μm , respectively. On the other hand, it was worth noting that the diameter distribution of the PVAc phase became wider with increasing PVAc content. The statistical results showed that for PBAT/PVAc blends, increasing dispersed phase content could lead to particle agglomeration, which is considerably influential with respect to mechanical behavior of polymer blends. Similar situation was also reported previously for PBAT blends with other polymers, such as poly(lactic acid) (PLA)/PBAT blends [56], PBAT/poly(glycolic acid) (PGA) [57] and PBAT/liquid crystalline polymer (LCP) [58]. For PLA/PBAT blends [56] with different weight ratio, all PLA/PBAT blends exhibited a typical two-phase structure and when the PBAT or PLA content was low, the size of the dispersed particles was small, and their distribution was relatively uniform. Increasing the content of dispersed phase in low content, the diameter of droplets grew gradually. For the PBAT/PGA blending system [57], as PGA content increased from 5 to 15 wt%, the particle sizes of PGA particles increased from 1.77 to 2.59 μm , like many

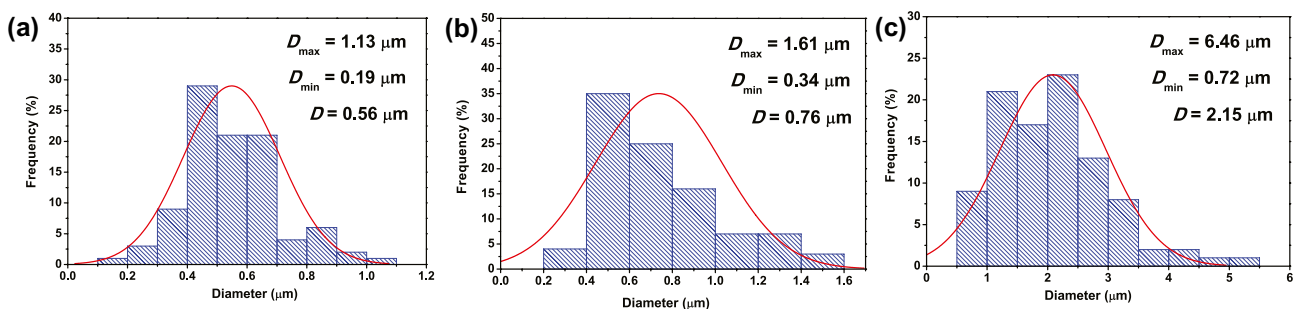


Fig. 5 Particle size distributions of PVAc phase based on the SEM images:(a) PBAT-10, (b) PBAT-20 and (c) PBAT-30

incompatible polymer blends, the size of the dispersed phase tends to increase with the increase of the dispersed phase content, due to development of breakdown and coalescence for the dispersed phase droplets. For the PBAT/LCP blends [58], typical sea-island morphologies were observed, in which LCP domains were precisely dispersed in the PBAT matrix and LCP domain size increased as the LCP composition increased.

Thermal behaviors

To investigate the thermal properties of PBAT/PVAc blends, DSC tests were carried out at a temperature rate of $10\text{ }^{\circ}\text{C min}^{-1}$. The DSC scanning thermograms of the first cooling runs and the second heating runs are shown in Fig. 6a, b, respectively. The related thermal parameters observed from DSC scanning thermograms are summarized in Table 2. The crystallization temperature peaks (T_c s) of neat PBAT and PBAT/PVAc blends were obviously observed and T_c of neat PBAT was $81.2\text{ }^{\circ}\text{C}$. However, with the incorporation of PVAc, T_c of PBAT showed a slight increased tendency for all PBAT/PVAc blends. For example, T_c was increased by about $3\text{ }^{\circ}\text{C}$ for sample of PBAT-30. This result indicated that the addition of PVAc could accelerate crystallization during cooling. The higher T_c indicated the nucleation of PBAT was promoted [59]. This observation may be a consequence of that amorphous PVAc could contribute to an increase of PBAT molecular chain mobility, and then crystallization ability of PBAT was enhanced.

From Fig. 6b (second heating runs), we can observe a T_g of neat PBAT at about $-34.6\text{ }^{\circ}\text{C}$ and a T_g of neat PVAc at about $44.0\text{ }^{\circ}\text{C}$. The T_g data obtained from DSC analysis were slightly different from DMA result (Table 1), which was resulted from different test methods used. For the PBAT/PVAc blends, two T_g s can be observed and two T_g s showed a slight change within the error range with the increase of PVAc content, which could declare that PBAT/PVAc blends were immiscible. These results were well consistent with the results obtained by DMA analysis.

The degree of crystallinity (X_c) of neat PBAT and PBAT/PVAc blends during crystallization were determined by the following equation and the results were listed in Table 2:

$$X_c = \frac{\Delta H_m}{w_{\text{PBAT}} \times \Delta H_m^0} \times 100\%$$

where X_c is the degree of crystallinity of PBAT phase, ΔH_m is the measured melting enthalpy, ΔH_m^0 is the heat of fusion for 100% crystalline PBAT (114 J g^{-1}) [60], and w_{PBAT} is the weight fraction of PBAT in the blends. From Table 2, it can be seen that X_c of neat PBAT was 5.7%. With the incorporation of PVAc, X_c also showed an increasing trend. The increase of X_c indicated that PVAc promoted

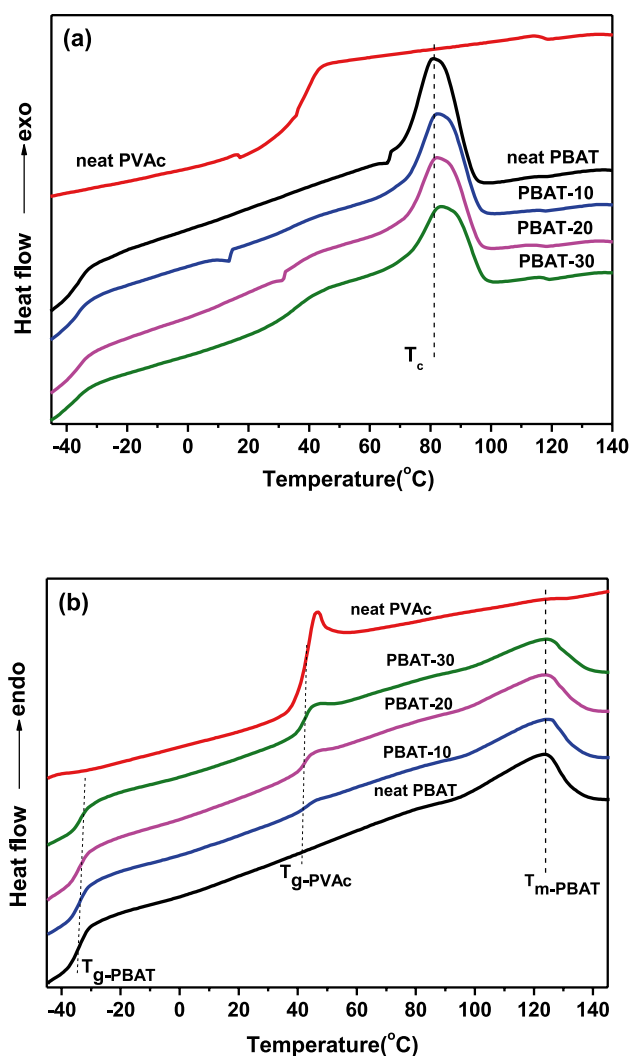


Fig. 6 DSC scanning thermograms of neat PBAT, neat PVAc and PBAT/PVAc blends: (a) the first cooling runs and (b) the second heating runs

PBAT molecular chain movement and, in consequence, the crystallization became easier. In addition, the incorporation of PVAc had no obvious effect on the T_m of PBAT in the blends. Zhang et al. [61] studied PBAT/poly(ethylene 2,5-furandicarboxylate) (PEF) blends and found that the addition of PEF enhanced the nucleation rate of PBAT from high temperature, and PEF should be a heterogeneous nucleating agent. However, PEF decreased the crystal growth rate of PBAT although it enhanced the nucleation rate of PBAT at high temperature. Similar to the result of our study is that PEF had no obvious effect on the T_m of PBAT in the blends. Hadj-Hamou et al. [42] used poly(vinyl chloride)(PVC) with the T_g of $85\text{ }^{\circ}\text{C}$ blended with PBAT. The difference with our study is that PBAT/PVC blends is miscible system with single glass transition temperature and the addition of PVC to PBAT matrix reduced the flexibility of PBAT. In

Table 2 Thermal and crystalline properties of neat PBAT, neat PVAc and PBAT/PVAc blends

Sample	T_{g-PBAT} (°C)	T_{g-PVAc} (°C)	T_c (°C)	T_m (°C)	ΔH_c (J/g)	ΔH_m (J/g)	X_c (%)
neat PBAT	-34.6	-	81.2	123.6	10.9	6.5	5.7
PBAT-10	-34.2	43.3	82.7	124.6	10.3	6.1	5.9
PBAT-20	-33.9	42.7	82.5	123.8	10.6	5.8	6.4
PBAT-30	-33.6	42.4	83.9	124.2	10.3	5.8	7.3
neat PVAc	-	44.0	-	-	-	-	-

addition, addition of PVC increased the glass transition temperature of PBAT and decreased the X_c due to the presence of strong interactions between the two polymers. Wu et al. [62] researched PBAT/poly(lactic acid) (PLA) blend with 80/20 wt% ratio and they found the melt crystallization rate of pure PLA was slow while PBAT had a fast melt crystallization rate. PBAT/PLA blend were immiscible with two T_g s showing no shift toward each other. The introduction of PLA could inhibit melt crystallization capability of PBAT due to a reduction in the lamellar thickness resulting from the melt blending. Moreover, T_m of PBAT/PLA blend had no apparent change compared with pure PBAT and PLA.

Rheological properties

Rheology can provide the information related to the processing parameters in polymer processing, hence the study of the rheological behavior is particularly important. In this section, dynamic rheological experiments carried out for the neat PBAT, neat PVAc, and PBAT/PVAc blends over the whole composition range were analyzed in detail. The storage modulus (G') represents the elastic character of blends or the energy stored in the deformation. The storage modulus versus angular frequency obtained from dynamic rheological experiment is shown in Fig. 7a. The G' increased with increasing angular frequency for all samples. It was seen that neat PVAc demonstrated an obvious pseudo-solid-like behavior at low-frequency zone with the slope of $\log(G')$ versus $\log(\omega)$ at low frequency region was 0.46, which mainly due to the high viscosity of PVAc in the melt state. It was noticed that neat PBAT exhibited a liquid-like behavior with the low frequency slope of $\log(G')$ versus $\log(\omega)$ was 1.5 and power-low dependence of the frequency. G' of neat PVAc was higher than those of neat PBAT and PBAT/PVAc blends in the whole range of frequencies tested. The G' of PBAT/PVAc blends increased with the PVAc content at lower frequencies region, which may be attributed to the increase in the PVAc dispersed phase domains size, similar behavior was observed for the PLA/ethylene vinyl acetate (EVA) blends [63]. As we all know that the greater is the dispersed phase domains size, the longer relaxation time, correspondingly, this results in an increase in G' at low frequencies [64–66]. Therefore, the increase of PVAc content

showed an increased elasticity of PBAT/PVAc blends. Analogous increases in G' in the frequency range studied have been reported for several PBAT blended with other polymer. For PBAT/poly(butylene succinate) (PBS) blends with crosslinking agent reported by Li et al. [67], likewise, the G' of PBAT/PBS blends increased with the PBS content at low frequencies region, while the slope of G' decreased. The larger G' means that the blends have a longer relaxation process which resulted from a higher degree of entangled network structure in blends system. In addition, similar tendency was observed for PBAT/poly(hydroxy amino ether) (PHAE) [68] and PBAT/poly(hydroxy ether of bisphenol A) (PH) blends [69]. In PBAT/PHAE system [68], the homopolymers exhibit a behavior close to that offered by the general linear viscoelastic mode, when PHAE was added into PBAT, the G' increased with the PHAE content and the blends deviate from this feature, due to the elasticity resulting from the interfacial tension between the two phases. For PBAT/PH system [69], PBAT shows the lowest G' values with a slope near 2 at the lower frequencies zone, a result which is practically in agreement with the linear viscoelastic model. On the other hand, PH shows high G' values in $\log G'$ - $\log \omega$ plots, with a slope considerably smaller than 2 at low frequencies G' and the slope of $\log G'$ - $\log \omega$ plots of PBAT/PH blend reduced increasing the content of PH, which is the responsible of hydrogen bonds. In PBAT/poly(vinyl alcohol) (PVA) blends [70], the G' of the PBAT/PVA blends increased with the additional PVA phase at the low sweep frequency. Meanwhile, at relatively high frequencies, the addition of PVA had less effect on the storage modulus of the melt due to the shortage of time for the entanglement recoveries. In our research, at higher frequencies region, no significant change of G' with increasing PVAc content was found. For PBAT/poly(propylene carbonate) (PPC) blends [71], the G' of PPC is higher than PBAT and the slope of the curve is smaller than PBAT at the low frequency range, which may be resulted from a higher viscosity of PPC than PBAT. When the PPC content added does not exceed 30%, the G' of PBAT-rich blends increased with PPC content increasing at lower frequencies region and the G' is almost unchanged with addition PPC at higher frequencies region. For PBAT/PLA stereocomplex (sc-PLA) blends [72], in the terminal (low frequency) zone, the PBAT melt demonstrated a typical liquid like

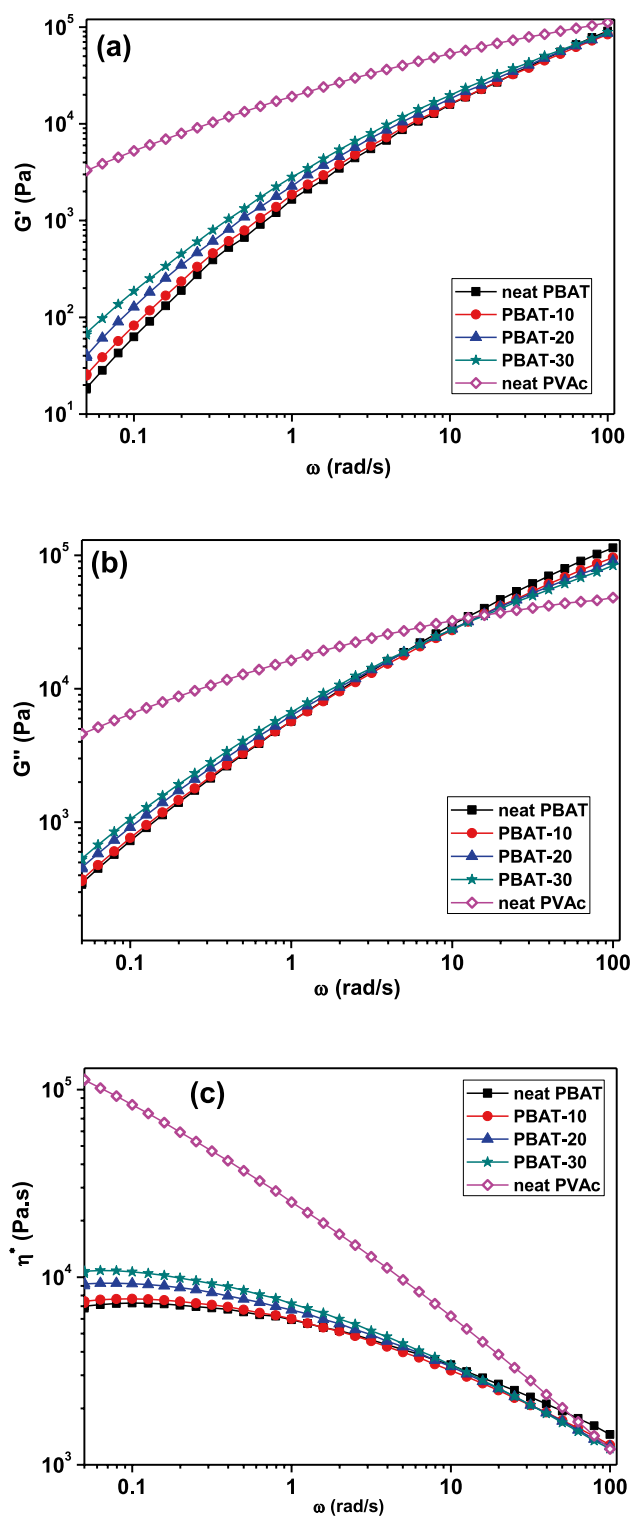


Fig. 7 Plots of (a): storage modulus (G'), (b): loss modulus (G''), (c): complex viscosity (η^*) versus angular frequency (ω) for neat PBAT, neat PVAc and PBAT/PVAc blends

behavior and logarithmic G' versus logarithmic ω showed a smooth linear relationship. G' increased with increasing sc-PLA concentration. However, G' is more sensitive to the

formation of sc-PLA than the addition of PVAc in our system, which could be due to the formed sc-crystallite network in PBAT/sc-PLA system. The above results indicate that the viscoelastic properties of these blends are significantly influenced by frequency and matrix.

Figure 7b shows the relationship between loss modulus (G'') and angular frequency. The loss modulus is related to the energy dissipated in the flow or the viscous character [73]. Similarly, G'' of all samples increased with angular frequency. In addition, G'' of PBAT/PVAc blends increased slightly with an increase in PVAc content at lower frequencies region, however, G'' of PBAT/PVAc blends decreased slightly with increase in PVAc content at higher frequencies region. This result was consistent with a simple linear mixing rule that it would be expected that the moduli for the blends would stand somewhere between those of PBAT and PVAc [74]. These results indicated that the addition of PVAc possessing high viscosity in the melt could enhance the melt strength of PBAT matrix. The G'' of PBAT/PVAc blends showed a trend similar to the PBAT/PVA blends [70] with low-composition PVA blends (i.e., 0–30 wt%), namely for PBAT/PVA and PBAT/PVAc blends, they have closed G'' values since the dispersed phase of PVA or PVAc molecules was relatively stiff.

The dependence of complex viscosity (η^*) on angular frequency is shown in Fig. 7c. As shown in Fig. 7c, like most pseudoplastic liquids, the η^* of neat PVAc exhibited a decrease with frequency increasing in the entire frequency range due to its considerably high viscosity, thus neat PVAc displayed typical non-Newtonian shear-thinning behavior. The η^* of neat PVAc was greater than that of PBAT and PBAT/PVAc blends over the entire frequency range. The pure PBAT and PBAT/PVAc blends displayed a Newtonian liquid behavior at low frequencies. Moreover, PBAT/PVAc blends showed smaller Newtonian platform when PVAc content was increased. Meanwhile, the addition of PVAc could increase the η^* of PBAT/PVAc blends only in small increments at low frequencies. Increment of viscosity results are benefit for blown film processing, because, the polymer melt extrudate should be stretched vertically before blowing and the increment of viscosity unfavored extrudate breaking. In the high frequency region, PVAc content had a less effect on the η^* of blends. The η^* of all blends decreased dramatically with frequency increasing because of the disentanglement of the chains and improved elastic response of the molecular chains in shorter time [75]. Similar tendency was observed in PBAT/PVA blends [70], the η^* of the PBAT and its blends decreased with increasing sweep frequency over the entire frequency range tested. The addition of the PVA phase in the blends shortened the Newtonian platform and enhanced the shear thinning behavior and the η^* differences among the blends decreased as the frequency increased in the relatively high

frequency ranges. These evolutions in η^* corresponded to morphology evolution. When the content of polymer additives is small, the morphology is dominated by sea-island structure, matrix governs the complex viscosity. When the content of polymer additives is big, morphology is dominated by co-continuous structure where both the polymers have three-dimensional spatial continuity forming an interpenetrated network structure, accordingly, both the two polymer phases contribute to the viscoelastic property. From SEM, we can know that PBAT/PVAc blends the morphology of PBAT/PVAc blends is dominated by sea-island structure, hence, all blends showed slightly increasing viscosity with the increasing of PVAc content, which is related to the higher complex viscosity of neat PVAc at low frequency.

The miscibility and phase morphology of polymer blends can be analyzed by Cole–Cole (η'' versus η') plot from the rheology testing to a certain extent. Cole–Cole plot is sensitive to the phase structures in polymer blends. If the Cole–Cole plot of polymer blends is smooth and semicircular, it could suggest that the polymers have good compatibility or the dispersed phase is uniform. If deviation from arc was observed, it could suggest that phase segregation occurs or dispersed phase is nonhomogeneous [76]. The Cole–Cole plots of the all samples are shown in Fig. 8a. As seen in Fig. 8a, neat PVAc showed a good linearity without any relaxation arc or tail, indicating its instantaneous relaxation. In contrast, the only semicircular arc in the curve of neat PBAT indicated good homogeneous structure relaxation of PBAT. For PBAT/PVAc blends, a single smooth circular arc without a tail observed implied that the minor PVAc phase uniformly distributed in PBAT matrix. These rheological results could be well consistent with the finely dispersive morphology observed by SEM. Interestingly, the radius of the arcs of PBAT/PVAc blends gradually became smaller when PBAT content increased, indicating short-time relaxation processes.

The loss tangent ($\tan\delta = G''/G'$) represents ratio of lost energy to stored energy in dynamic condition, which can characterize the relaxation process of viscoelastic material. The $\tan\delta$ value as a function of frequency is illustrated in Fig. 8b. The curves of all samples had negative slope over tested frequency range and the $\tan\delta$ decreased with increasing frequency, a straight line in the whole frequency range was even observed at all PVAc content, indicating typical viscoelastic liquids. With an increase in PVAc content, the $\tan\delta$ curves of PBAT/PVAc blends showed a decreased tendency, which indicated that a much larger elastic contribution to melt strength than viscous contribution, and the incorporation of PVAc enhanced the elastic behavior of blends melt due to its high viscosity.

Figure 8c shows the Van Gorp–Palmen curves of all samples, which is a plot of phase angle (δ) versus complex

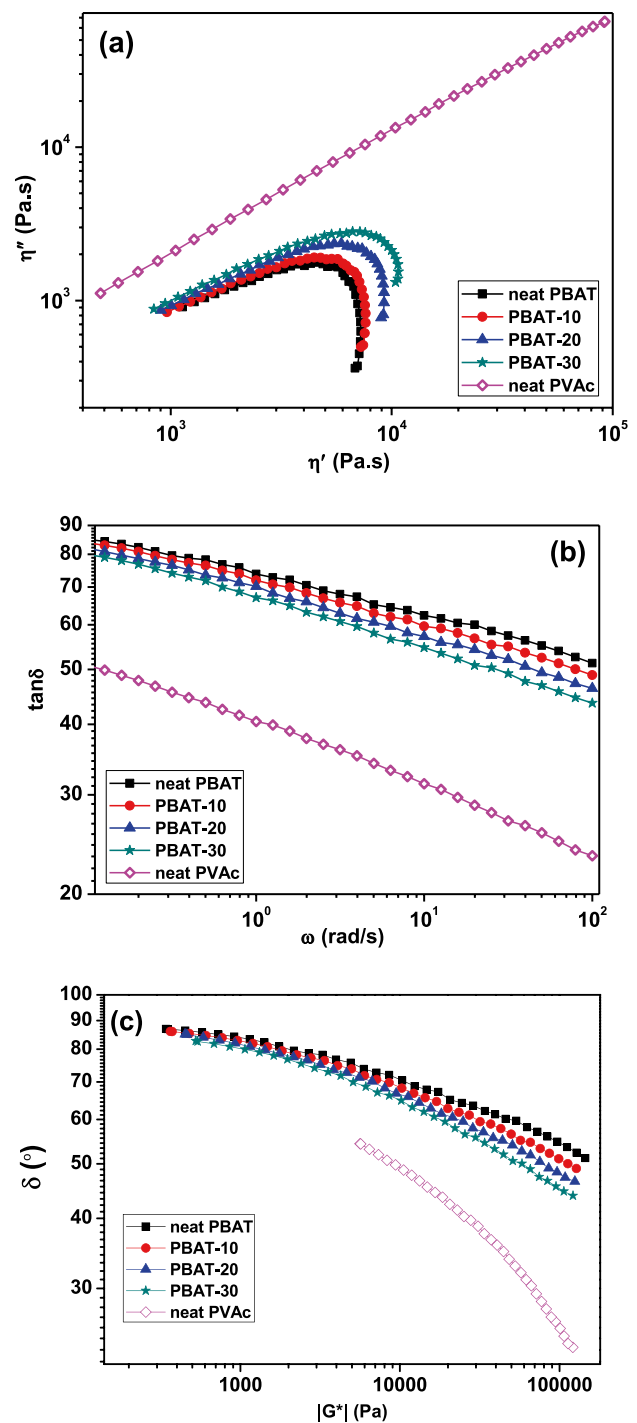


Fig. 8 Plots of (a) cole–cole plots, (b) $\tan\delta$ versus angular frequency (ω) and (c) Van Gorp–Palmen curves for neat PBAT, neat PVAc and PBAT/PVAc blends

modulus $|G^*|$. Low δ value means that the material has great elasticity. Pure PBAT showed a δ value of 88° in the low $|G^*|$, indicating its viscoelastic fluid behavior. The δ value at low $|G^*|$ for pure PVAc was about 55° , suggesting the high

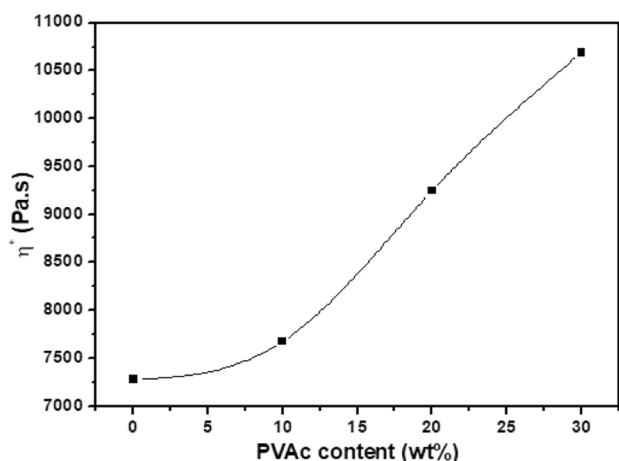


Fig. 9 Complex viscosity versus PVAc content at frequency of 0.1 s^{-1}

elasticity of PVAc melt. With the increase of PVAc content, the δ value of PBAT/PVAc blends at low $|G^*|$ decreased slightly, indicating that the effect of PVAc on the elasticity enhancement of PBAT was not obvious due to the immiscibility of PVAc and PBAT.

The results of linear viscoelastic studies, applied in small amplitudes, can provide reliable information on microstructure of the blends, which due to the effect of flow induced molecular orientation on viscosity and elasticity becomes more less at low frequencies. The complex viscosity versus blend composition at angular frequency of 0.1 s^{-1} is presented in Fig. 9. As can be seen from the Fig. 9, with PVAc content increasing, the complex viscosity of the blend showed an increasing trend. The effect of mixing condition on microstructure of the blends was investigated by SEM among PBAT-20 prepared at $130 \text{ }^\circ\text{C}$, $150 \text{ }^\circ\text{C}$ and $170 \text{ }^\circ\text{C}$, and then the effect of blend morphology on rheological properties was studied. Figure 10 showed SEM images of PBAT-20 prepared at $130 \text{ }^\circ\text{C}$, $150 \text{ }^\circ\text{C}$ and $170 \text{ }^\circ\text{C}$ and Fig. 11 showed the rheological results. It was seen that the mixing temperature do not have a significant effect on the

final morphology of the blends, the particle size of PVAc dispersed phase changed very little. Accordingly, the rheological properties of the blend had little change, as shown in Fig. 11. This result signified that the PBAT/PVAc blend system has a wide range of processing temperature and relatively stable morphology rheological properties, which is beneficial to its processing production and widens the melt processing window. Similar research had reported in PBAT/poly(ethylene-co-vinyl alcohol) (EVOH) blend system [77], when EVOH content was fixed, blending conditions such as blending temperature, mixing time and rotor speed were changed, as a result the morphology of blending changed with difference in particle size of dispersed phase, and no significant change is observed for rheological properties such as G'' , G' and η^* .

Comprehensive results of rheological behavior study indicated the addition of PVAc not only benefit for blown film processing, but also is favorable to foaming. The storage modulus (G') which represents the elastic character of blends is one of the important indexes to measure the foamability of blend system. The higher G' is, the better the melt elasticity of the blend system is, accordingly the higher the melt strength of the blend system is, and the better the foamability is. Large elasticity over viscosity is favorable to CO_2 foaming for bubble stabilization [78]. In addition, $\tan\delta$ is the phase difference between the strain and the stress of the melt under the action of alternating stress. The smaller $\tan\delta$ value is, the smaller the phase difference is, the faster the elastic response of the blend system is, the less viscous dissipation is, and the better the foamability is. In the actual production process, the shear rate of melt is in the low-frequency region, so we mainly analyze the rheological behavior in the low-frequency region. Based on the rheological results obtained from the previous analysis, we know that the G' of neat PBAT was lower than those of other PBAT/PVAc blends in the low-frequency region. At the same shear frequency, the G' of PBAT/PVAc blends increased slightly with an increase of PVAc content, which indicated that addition of PVAc could improve the melt elasticity of PBAT, thus the melt

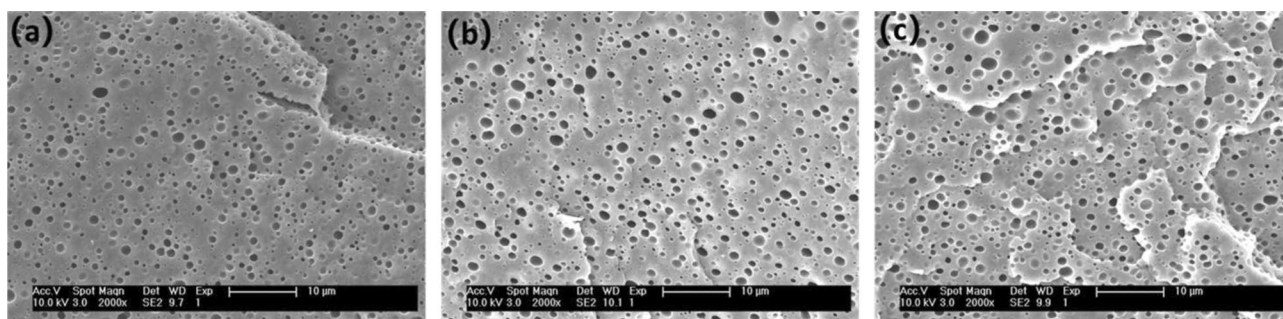


Fig. 10 SEM images of cryo-fractured surfaces of PBAT-20 blend after etching PVAc: (a) blending at $130 \text{ }^\circ\text{C}$ (b) blending at $150 \text{ }^\circ\text{C}$ (c) blending at $170 \text{ }^\circ\text{C}$

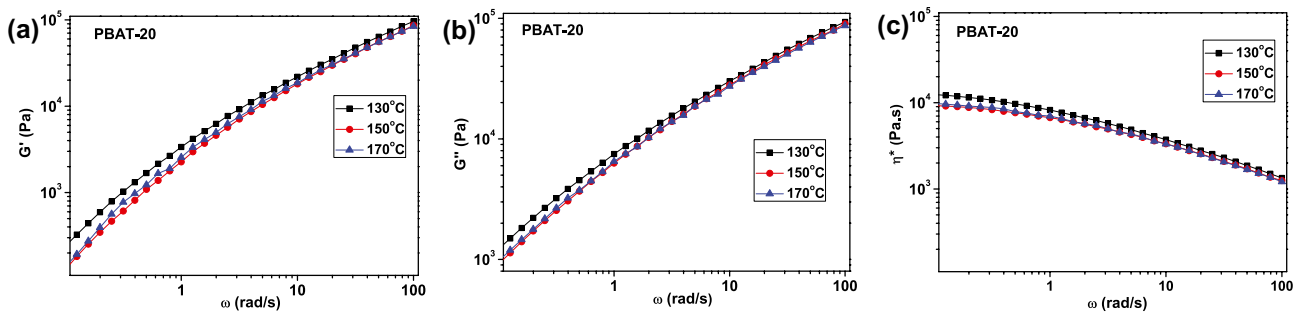


Fig. 11 The rheological results for PBAT-20 at different blending temperature: plots of (a), storage modulus (G') (b), loss modulus (G'') (c), complex viscosity (η^*) versus angular frequency (ω)

strength could be improved. The end result is an improvement in the foamability of PBAT. In terms of $\tan\delta$ analysis, in the low frequency region, when the shear frequency was constant, the $\tan\delta$ value of pure PBAT was the highest, indicating that its elastic response was slow and viscosity dissipation phenomenon was obvious, thus its foamability was not ideal. After PVAc was added, $\tan\delta$ values of PBAT/PVAc blend system in low frequency region decreased, indicating that the elastic strain of the blend system was fast, viscosity dissipation phenomenon was gradually reduced, and the foamability was improved.

Tensile mechanical properties

The results obtained from the typical tension stress–strain curves are depicted in Fig. 12. Table 3 summarizes the relative mechanical properties including Young's modulus, yield strength, tensile strength, and elongation at break. From Fig. 12, we can conclude that all samples showed toughness fracture upon tensile load with obvious strain hardening behavior. With the regard to the PBAT-30, a longer neck growth was clearly observed compared with the other samples. For neat PBAT, it had a low Young's modulus about 203 MPa and a high elongation at break about 1471%. In addition, neat PBAT exhibited the yield strength and tensile strength of 7.5 and 37.3 MPa, respectively. It is observed that the incorporation of PVAc can obviously affect mechanical properties of PBAT. Figure 12 obviously revealed that tensile strength (breaking stress) and elongation at break of samples declined with the increase of PVAc content. This result may be due to the phase separation caused by the immiscibility of PBAT and PVAc. However, the yield stress and Young's modulus of samples were enhanced with increasing PVAc content. The Young's modulus represents the stiffness of material. Young's modulus was improved about 105% when PVAc content was 30% (from 203 to 416 MPa), which indicated that incorporation of PVAc could make up for the shortcoming of low modulus of PBAT. Moreover, yield strength was significantly improved about

53.3% (from 7.5 to 11.5 MPa) when PVAc content was 30%. The Young's modulus and yield strength of the PBAT/PVAc blends were higher than those of neat PBAT, which could result from a relatively high hardness of PVAc at room temperature caused by its higher T_g than PBAT. Although the elongation at break decreased with PVAc content increasing,

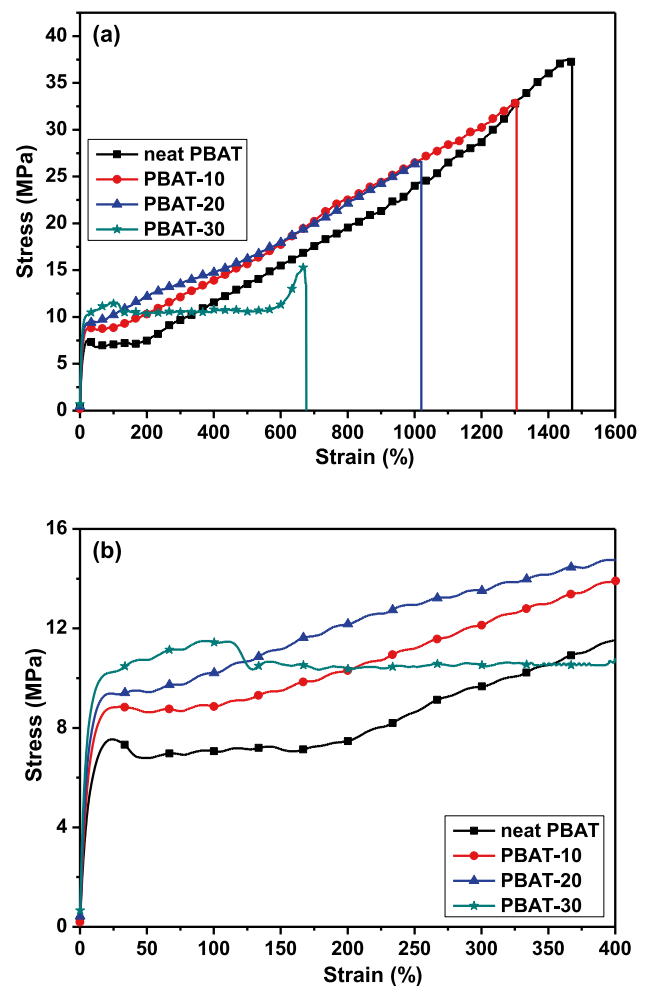


Fig. 12 (a) tensile behavior of neat PBAT and PBAT/PVAc blends; (b) the magnified tensile behavior

Table 3 Mechanical properties of neat PBAT and PBAT/PVAc blends

Sample	Young's modulus (MPa)	Yield strength (MPa)	Tensile strength (MPa)	Elongation at break (%)
neat PBAT	203 ± 23	7.5 ± 0.4	37.3 ± 1.9	1471 ± 56
PBAT-10	228 ± 14	8.9 ± 0.5	33.2 ± 1.4	1305 ± 42
PBAT-20	284 ± 21	9.4 ± 0.6	27.8 ± 0.8	1020 ± 31
PBAT-30	416 ± 34	11.5 ± 0.3	16.9 ± 0.5	713 ± 23

all the PBAT/PVAc blends with various PVAc content maintained the elongation at break of more than 700%, which meets the requirements of most applications. Compared with PBAT/PVC researched by Hadj-Hamou et al. [42], when PVAc and PVC content is 30wt%, Young's modulus, tensile strength and elongation at break of PBAT/PVAc blend were 416 MPa, 16.9 MPa and 713%, respectively, while Young's modulus, tensile strength and elongation at break of PBAT/PVC blend were 103 MPa, 19.2 MPa and 383%, respectively. The above results indicated that PVAc has better enhancement effect on PBAT than PVC. Iwakura et al. [58] have been studied PBAT melt-blended with a liquid crystalline polymer (LCP) aiming at improving mechanical properties and the result showed that the addition of LCP to PBAT increased tensile strength and tensile modulus. However, unlike our PBAT/PVAc blends, no tensile yield points can be observed in PBAT/LCP blends. Zhao et al. [36] have been studied PBAT/PPC blends and the PPC content has a significant effect on mechanical properties, such as both tensile strength and tensile modulus decreased with PPC content increasing. When PPC content was 10%, 20% and 30%, the tensile strength and elongation at break of PBAT/PPC blends were 30.2 MPa/1553%, 26.0 MPa/1473% and 19.5 MPa/1184%, respectively. In our PBAT/PVAc blends, the tensile strength and elongation at break of PBAT/PVAc blends were 33.2 MPa/1305%, 27.8 MPa/1020% and 16.9 MPa/713%, respectively. This result indicated that the effects of PPC and PVAc on PBAT mechanics have similar results. They also found a small amount of chain extender ADR could improve mechanical properties of PBAT/PPC blends. Elhamnia et al. [77] studied mechanical properties of melt-mixed PBAT/EVOH blends with 10%, 20%, 30% EVOH content, they found that the yield stress and strain at yield of the blends were not greatly affected by the EVOH content. Moreover, strain at break has slightly decreased with a large drop at 30% EVOH but tensile strength decreased with increasing EVOH content. For PBAT/EVOH and PBAT/PVAc blend, the decrease of tensile strength and strain at break of the blends probably because that EVOH or PVAc droplets were relatively stiff and stiff droplets as dispersed phase could inhibit the elongation of PBAT chains by defects developed at the interface and consequently strain at break decreases and strain hardening of PBAT continuous

phase become weak [77]. The decrease of tensile strength and strain at break of the blends is more pronounced when the EVOH or PVAc content increase.

From the analysis of mechanical properties, it can be seen that the addition of PVAc can effectively improve the mechanical properties of PBAT, which is conducive to the application of blends in film and foam. The improvement of the modulus and strength could make the blend film more solid and do not happen destructive deformation easily and endows foaming with certain strength.

Conclusions

In this work, PBAT/PVAc blends with different PVAc contents were successfully produced by a sample melt blending method. A comprehensive and detailed analysis of the blends was investigated through the combination of the miscibility, phase morphology, thermal behaviors, rheological and mechanical properties. DMA result indicated that PBAT and PVAc were immiscible and PBAT/PVAc blends presented two glass transition temperatures. Morphological analysis demonstrated phase separation existed in the PBAT/PVAc blends and PVAc minor phase uniformly dispersed in the PBAT matrix in our study range. From thermal behaviors analysis, we found that T_c value of PBAT was increased when PVAc was added and PVAc could accelerate crystallization during cooling. In addition, degree of crystallinity of PBAT was increased with the incorporation of PVAc increasing. However, the addition of PVAc did not affect the melting temperature of PBAT. Rheological properties tests showed that the storage modulus, loss modulus, and complex viscosity of PBAT/PVAc blends were increased with the PVAc content and this was attributed to fact that the higher viscosity of PVAc. On the basis of the tensile test results, upon the increasing PVAc content, PBAT/PVAc blends displayed a decrease in elongation at break and tensile strength, while Young's modulus and yield strength were gradually improved. In summary, the improvement of rheological and mechanical properties for PBAT/PVAc blend can augment the performance of its products and expand its wider market applications in film and foam fields.

Acknowledgements This work is supported by the Chinese Academy of science and technology service network planning (KFJ-STS-QYZD-140).

Declarations

Conflict of interest There are no conflicts of interest to disclose.

References

- Lyu Y, Chen Y, Lin Z, Zhang J, Shi X (2020) Manipulating phase structure of biodegradable PLA/PBAT system: Effects on dynamic rheological responses and 3D printing. *Compos Sci Technol* 200:108399
- Kumar M, Mohanty S, Nayak SK, Parvaiz MR (2010) Effect of glycidyl methacrylate (GMA) on the thermal, mechanical and morphological property of biodegradable PLA/PBAT blend and its nanocomposites. *Bioresour Technol* 101:8406–8415
- Roy S, Rhim JW (2020) Curcumin incorporated poly(Butylene adipate-co-terephthalate) film with improved water vapor barrier and antioxidant properties. *Materials* 13:4369
- Yasin S, Hussain M, Zheng Q, Song Y (2021) Large amplitude oscillatory rheology of silica and cellulose nanocrystals filled natural rubber compounds. *J Colloid Interface Sci* 588:602–610
- Silva-Guzman JA, Rodriguez Anda R, Fuentes-Talavera FJ, Manriquez-Gonzalez R, Lomeli-Ramirez MG (2018) Properties of thermoplastic corn starch based green composites reinforced with barley (*hordeum vulgare* L.) straw particles obtained by thermal compression. *Fiber Polym* 19:1970–1979
- Chaikeaw C, Srikulkit K (2018) Preparation and properties of poly(lactic acid)/PLA-g-ABS blends. *Fiber Polym* 19:2016–2022
- Takkalkar P, Griffin G, Kao N (2019) Enhanced mechanical and barrier performance of poly (lactic acid) based nanocomposites using surface acetylated starch nanocrystals. *J Polym Environ* 27:2078–2088
- Srisa A, Harnkarnsujarit N (2020) Antifungal films from trans-cinnamaldehyde incorporated poly(lactic acid) and poly(butylene adipate-co-terephthalate) for bread packaging. *Food Chem* 333:127537
- Luzi F, Fortunati E, Jimenez A, Puglia D, Pezzolla D, Gigliotti G, Kenny JM, Chiralt A, Torre L (2016) Production and characterization of PLA_PBS biodegradable blends reinforced with cellulose nanocrystals extracted from hemp fibres. *Ind Crop Prod* 93:276–289
- Carrasco F, Pages P, Gamez-Perez J, Santana OO, MasPOCH ML (2010) Kinetics of the thermal decomposition of processed poly(lactic acid). *Poly Degrad Stabil* 95:2508–2514
- Suzuki M, Tachibana Y, Kasuya KI (2021) Biodegradability of poly(3-hydroxyalkanoate) and poly(epsilon-caprolactone) via biological carbon cycles in marine environments. *Polym J* 53:47–66
- Naik S, Gopal SKV, Somal P (2008) Bioproduction of polyhydroxyalkanoates from bacteria: a metabolic approach. *World J Microb Biot* 24:2307–2314
- Ding Y, Zhou Q, Han A, Zhou H, Chen R, Guo S (2020) Fabrication of poly(epsilon-caprolactone)-based biodegradable packaging materials with high water vapor barrier property. *Ind Eng Chem Res* 59:22163–22172
- Garcia-Garcia D, Ferri JM, Boronat T, Lopez-Martinez J, Balart R (2016) Processing and characterization of binary poly(hydroxybutyrate) (PHB) and poly(caprolactone) (PCL) blends with improved impact properties. *Polym Bull* 73:733333–733350
- Zhang C, Lan Q, Zhai T, Nie S, Luo J, Yan W (2018) Melt crystallization behavior and crystalline morphology of polylactide/poly(epsilon-caprolactone) blends compatibilized by lactide-caprolactone copolymer. *Polymers* 10:1181
- Song CL, Jiang BZ, Fumio Y (2001) Radiation crosslinking of biodegradable poly(butylene succinate) and its heat distortion behavior. *Acta Polym Sin*:691–693
- He Z, Liang Y, Han CC (2013) Confined nucleation and growth of poly(ethylene oxide) on the different crystalline morphology of poly(butylene succinate) from a miscible blend. *Macromolecules* 46:8264–8274
- Wang HM, Wang B, Yuan TQ, Zheng L, Shi Q, Wang SF, Song GY, Sun RC (2020) Tunable, UV-shielding and biodegradable composites based on well-characterized lignins and poly(butylene adipate-co-terephthalate). *Green Chem* 22:8623–8632
- Herrera R, Franco L, Rodriguez-Galan A, Puiggali J (2002) Characterization and degradation behavior of poly(butylene adipate-co-terephthalate)s. *J Polym Sci Pol Chem* 40:4141–4157
- Zhu K, Zhu WP, Gu YB, Shen ZQ, Chen W, Zhu GX (2007) Synthesis and characterization of poly(butylene adipate-co-terephthalate) catalyzed by rare earth stearates. *Chinese J Chem* 25:1581–1583
- Chen Y, Xie K, He Y, Hu W (2021) Fast-scanning chip-calorimetry measurement of crystallization kinetics of poly(glycolic acid). *Polymers* 13:891
- Yeo T, Ko YG, Kim EJ, Kwon OK, Chung HY, Kwon OH (2021) Promoting bone regeneration by 3D-printed poly(glycolic acid)/hydroxyapatite composite scaffolds. *J Ind Eng Chem* 94:343–351
- Cho JS, Hayashino Y, Miyatake K, Takeoka S, Tsuchida E (2000) Proton-conduction of perfluorooctanesulfonic acid/poly(propylene carbonate) composites. *Chem Lett* 44–45
- Xy W, Xq D, Yang N, Yx W, Wang W (2015) Chain extension and modification of polypropylene carbonate using diphenylmethane diisocyanate. *Polym Int* 64:1491–1496
- Wei D, Wang H, Xiao H, Zheng A, Yang Y (2015) Morphology and mechanical properties of poly(butylene adipate-co-terephthalate)/potato starch blends in the presence of synthesized reactive compatibilizer or modified poly(butylene adipate-co-terephthalate). *Carbohydr Polym* 123:275–282
- Pal AK, Wu F, Misra M, Mohanty AK (2020) Reactive extrusion of sustainable PHBV/PBAT-based nanocomposite films with organically modified nanoclay for packaging applications: Compression moulding vs. cast film extrusion. *Compos Part B-Eng* 198:108141
- Bang YJ, Shankar S, Rhim JW (2020) Preparation of polypropylene/poly (butylene adipate-co-terephthalate) composite films incorporated with melanin for prevention of greening of potatoes. *Packag Technol Sci* 33:433–441
- Xing Q, Buono P, Ruch D, Dubois P, Wu L, Wang WJ (2019) Biodegradable UV-blocking films through core-shell lignin-melanin nanoparticles in poly(butylene adipate-co-terephthalate). *ACS Sustain Chem Eng* 7:4147–4157
- Jiang L, Wolcott MP, Zhang JW (2006) Study of biodegradable polylactide/poly(butylene adipate-co-terephthalate) blends. *Biomacromol* 7:199–207
- Han Y, Shi J, Mao L, Wang Z, Zhang L (2020) Improvement of compatibility and mechanical performances of PLA/PBAT composites with epoxidized soybean oil as compatibilizer. *Ind Eng Chem Res* 59:21779–21790
- Teamsinsungvon A, Ruksakulpiwat Y, Jarukumjorn K (2013) Preparation and characterization of poly(lactic acid)/poly(butylene adipate-co-terephthalate) blends and their composite. *Polym-Plast Technol* 52:1362–1367
- Brandelero RPH, Grossmann MV, Yamashita F (2012) Films of starch and poly(butylene adipate co-terephthalate) added of soybean oil (SO) and Tween 80. *Carbohydr Polym* 90:1452–1460

33. Nayak SK (2010) Biodegradable PBAT/starch nanocomposites. *Polym-Plast Technol* 49:1406–1418
34. Stagner JA, Alves VD, Narayan R (2012) Application and performance of maleated thermoplastic starch-poly(butylene adipate-co-terephthalate) blends for films. *J Appl Polym Sci* 126:E135–E142
35. Bai J, Pei H, Zhou X, Xie X (2021) Reactive compatibilization and properties of low-cost and high-performance PBAT/thermoplastic starch blends. *Eur Polym J* 143:110198
36. Zhao Y, Li Y, Xie D, Chen J (2021) Effect of chain extender on the compatibility, mechanical and gas barrier properties of poly(butylene adipate-co-terephthalate)/poly(propylene carbonate) bio-composites. *Appl Polym Sci* 138:e50487
37. de Matos Costa AR, Crocitti A, Hecker de Carvalho L, Carroccio SC, Cerruti P, Santagata G (2020) Properties of biodegradable films based on poly(butylene Succinate) (PBS) and poly(butylene Adipate-co-Terephthalate) (PBAT) blends. *Polymers* 12:2317
38. Pawar SP, Misra A, Bose S, Chatterjee K, Mittal V (2015) Enzymatically degradable and flexible bio-nanocomposites derived from PHBV and PBAT blend: Assessing thermal, morphological, mechanical, and biodegradation properties. *Colloid Polym Sci* 293:2921–2930
39. Pagno V, Modenes AN, Dragunski DC, Fiorentin-Ferrari LD, Caetano J, Guellis C, Goncalves BC, dos Anjos EV, Pagno F, Martinelli V (2020) Heat treatment of polymeric PBAT/PCL membranes containing activated carbon from Brazil nutshell biomass obtained by electrospraying and applied in drug removal. *J Environ Chem Eng* 8:104159
40. Wang R, Sun X, Chen L, Liang W (2021) Morphological and mechanical properties of biodegradable poly(glycolic acid)/poly(butylene adipate-co-terephthalate) blends with in situ compatibilization. *RSC Adv* 11:1241–1249
41. Dhandapani S, Nayak SK, Mohanty S (2016) Analysis and evaluation of biobased polyester of PTT/PBAT blend: Thermal, dynamic mechanical, interfacial bonding, and morphological properties. *Polym Advan Technol* 27:938–945
42. Hadj-Hamou AS, Matassi S, Abderrahmane H, Yahiaoui F (2014) Effect of cloisite 30B on the thermal and tensile behavior of poly(butylene adipate-co-terephthalate)/poly(vinyl chloride) nanoblends. *Polym Bull* 71:1483–1503
43. Lule ZC, Kim J (2021) Compatibilization effect of silanized SiC particles on polybutylene adipate terephthalate/polycarbonate blends. *Mater Chem Phys* 258:123879
44. Kalkornsurapranee E, Koedthip D, Songtipya P, Prodpran T, Johns J, Nakaramontri Y, Songtipya L (2020) Influence of modified natural rubbers as compatibilizers on the properties of flexible food contact materials based on NR/PBAT blends. *Mater Design* 196:109134
45. Titone V, La Mantia FP, Mistretta MC (2020) The Effect of calcium carbonate on the photo-oxidative behavior of poly(butylene adipate-co-terephthalate). *Mater Eng* 305:2000358
46. Geng S, Shah FU, Liu P, Antzutkin ON, Oksman K (2017) Plasticizing and crosslinking effects of borate additives on the structure and properties of poly(vinyl acetate). *RSC Adv* 7:7483–7491
47. Corrales TP, Laroze D, Zardalidis G, Floudas G, Butt HJ, Kappl M (2013) Dynamic heterogeneity and phase separation kinetics in miscible poly(vinyl acetate)/poly(ethylene oxide) blends by local dielectric spectroscopy. *Macromolecules* 46:7458–7464
48. Sivalingam G, Karthik R, Madras G (2004) Blends of poly(epsilon-caprolactone) and poly(vinyl acetate): Mechanical properties and thermal degradation. *Polym Degrad Stabil* 84:345–351
49. Gajria AM, Dave V, Gross RA, McCarthy SP (1996) Miscibility and biodegradability of blends of poly(lactic acid) and poly(vinyl acetate). *Polymer* 37:437–444
50. Li Y, Han C, Xiao L, Yu Y, Zhou G, Xu M (2021) Miscibility, morphology, and properties of poly(butylene succinate)/poly(vinyl acetate) blends. *Colloid Polym Sci* 299:105–116
51. Guo QP, Liu ZH (2000) Phase behavior of polymer blends. *J Therm Anal Calorim* 59:101–120
52. Kumagai Y, Doi Y (1992) Enzymatic degradation and morphologies of binary blends of microbial poly(3-hydroxy butyrate) with poly(epsilon-caprolactone), poly(1,4-butylene adipate and poly(vinyl acetate)). *Polym Degrad Stabil* 36:241–248
53. Aravind I, Boumod A, Grohens Y, Thomas S (2010) Morphology, dynamic mechanical, thermal, and crystallization behaviors of poly(trimethylene terephthalate)/polycarbonate blends. *Ind Eng Chem Res* 2010:3873–3882
54. Muthuraj R, Misra M, Mohanty AK (2014) Biodegradable poly(butylene succinate) and poly(butylene adipate-co-terephthalate) blends: Reactive extrusion and performance evaluation. *J Polym Environ* 22:336–349
55. Hu X, Li Y, Li M, Kang H, Zhang L (2016) Renewable and super-toughened polylactide-based composites: Morphology, interfacial compatibilization, and toughening mechanism. *Ind Eng Chem Res* 55:9195–9204
56. Su S, Duhme M, Kopitzky R (2020) Uncompatibilized PBAT/PLA blends: Manufacturability, miscibility and properties. *Materials* 13:4897
57. Shen JN, Wang K, Ma Z, Xu N, Pang SJ, Pan LS (2021) Biodegradable blends of poly(butylene adipate-co-terephthalate) and polyglycolic acid with enhanced mechanical, rheological and barrier performances. *Appl Polym Sci* 138:e51285
58. Iwakura Y, Li YJ, Nakayama K, Shimizu H (2008) Strengthening of poly(butylene adipate-co-terephthalate) by melt blending with a liquid crystalline polymer. *J Appl Polym Sci* 109:333–339
59. Li X, Tan D, Xie L, Sun H, Sun S, Zhong G, Ren P (2018) Effect of surface property of halloysite on the crystallization behavior of PBAT. *Appl Clay Sci* 157:218–226
60. Ravati S, Beaulieu C, Zolali AM, Favis BD (2014) High performance materials based on a self-assembled multiple-percolated ternary blend. *Aiche J* 60:3005–3012
61. Zhang Q, Jiang M, Zhou GY (2020) Novel biobased high toughness PBAT/PEF blends: Morphology, thermal properties, crystal structures and mechanical properties. *New J Chem* 44:3112–3121
62. Wu DD, Guo Y, Huang AP, Xu RW, Liu P (2020) Effect of the multi-functional epoxides on the thermal, mechanical and rheological properties of poly(butylene adipate-co-terephthalate)/polylactide blends. *Polym Bull* 78:5567–5591
63. Agrawal P, Araujo APM, Lima JCC, Cavalcanti SN, Freitas DMG, Farias GMG, Ueki MM, Melo TJA (2019) Rheology, mechanical properties and morphology of poly(lactic acid)/ethylene vinyl acetate blends. *J Polym Environ* 27:1439–1448
64. Yee M, Calvao PS, Demarquette NR (2007) Rheological behavior of poly(methyl methacrylate)/polystyrene (PMMA/PS) blends with the addition of PMMA-ran-PS. *Rheol Acta* 46:653–664
65. Calvao PS, Yee M, Demarquette NR (2005) Effect of composition on the linear viscoelastic behavior and morphology of PMMA/PS and PMMA/PP blends. *Polymer* 46:2610–2620
66. Wu DF, Zhang YS, Zhang M, Zhou WD (2008) Phase behavior and its viscoelastic response of polylactide/poly(epsilon-caprolactone) blend. *Eur Polym J* 44:2171–2183
67. Li YT, Zhang ZY, Wang WM, Gong PJ, Yang Q, Park CB, Li GX (2022) Ultra-fast degradable PBAT/PBS foams of high performance in compression and thermal insulation made from environment-friendly supercritical foaming. *J Supercrit Fluid* 181:105512
68. Sangroniz A, Sangroniz L, Etxeberria A (2018) Blends of biodegradable poly(butylene adipate-co-terephthalate) with poly(hydroxi amino ether) for packaging applications: Miscibility, rheology and transport properties. *Eur Polym J* 105:348–358
69. Sangroniz A, Sangroniz L, Gonzalez A, Santamaria A, del Rio J, Iriarte M, Etxeberria A (2019) Improving the barrier properties of

- a biodegradable polyester for packaging applications. *Eur Polym J* 115:76–85
70. Peng J, Zhang CM, Mi HY, Peng XF, Turng LS (2014) Study of solid and microcellular injection-molded poly(butylene adipate-co-terephthalate)/poly(vinyl alcohol) biodegradable parts. *Ind Eng Chem Res* 53:8493–8500
 71. Jiang G, Wang F, Zhang SD, Huang HX (2020) Structure and improved properties of PPC/PBAT blends via controlling phase morphology based on melt viscosity. *Appl Polym Sci* 37:48924
 72. Shi XT, Qin JB, Wang L, Ren LC, Rong F, Li DH, Wang R, Zhang GC (2018) Introduction of stereocomplex crystallites of PLA for the solid and microcellular poly(lactide)/poly(butylene adipate-co-terephthalate) blends. *RSC Adv* 8:11850–11861
 73. Ding Y, Lu B, Wang PL, Wang GX, Ji JH (2018) PLA-PBAT-PLA tri-block copolymers: Effective compatibilizers for promotion of the mechanical and rheological properties of PLA/PBAT blends. *Polym Degrad Stabil* 147:41–48
 74. Cunha M, Fernandes B, Covas JA, Vicente AA, Hilliou L (2016) Film blowing of PHBV blends and PHBV-based multilayers for the production of biodegradable packages. *J Appl Polym Sci* 133:42165
 75. Xu XL, Chen JZ, An LJ (2014) Shear thinning behavior of linear polymer melts under shear flow via nonequilibrium molecular dynamics. *J Chem Phys* 140:174902
 76. Meng B, Deng J, Liu Q, Wu Z, Yang W (2012) Transparent and ductile poly(lactic acid)/poly(butyl acrylate) (PBA) blends: Structure and properties. *Eur Polym J* 48:127–135
 77. Elhamnia M, Motlagh GH, Jafari SH (2020) A multiple approach in determination of interfacial tension of biodegradable melt-mixed PBAT/EVOH blends: Correlation of morphology, rheology and mechanical properties. *Polym Test* 82:106301
 78. Richard G, Caroline V (2003) Effect of viscosity on low density foaming of poly(ethylene-co-octene) resins. *J Cell Plast* 39:117–132

Publisher's Note Springer Nature remains neutral with regard to jurisdictional claims in published maps and institutional affiliations.